2015 IEEE 54th Annual Conference on Decision and Control (CDC)
December 15-18, 2015. Osaka, Japan

Data Driven Predictive Control Based on Orthonormal Basis Functions

A.A.Bachnas, S.Weiland, and R Tóth

Abstract— **This paper presents a concept of an adaptive *model predictive control* (MPC) scheme based on a flexible predictor model that utilizes *orthonormal basis functions* (OBFs). This model structure offers a trade-off between adaptation of the model accuracy in terms of the expansion coefficients and the dynamical structure in terms of the basis functions. We show that this adaptation can maintain desirable control performance. Moreover, since OBF model structures can be seen as a generalization of *finite impulse response* (FIR) model structures, the incorporation of this scheme in FIR-based MPC is rather straightforward.**

I. Introduction

Model predictive control (MPC) is widely applied in the process control field [1]. This control scheme allows safe operation of the controlled plant subject to boundary and operational conditions. However, due to wear in the process and possible changes in the operational conditions, the desired performance of the controller can only be sustained in a limited time period after its commissioning. Such problems are either solved by enforcing the MPC to be robust w.r.t. all possible changes of operational conditions and disturbances, or by equipping the MPC with adaptation capabilities. In contrast with the research in robust MPC, a recent survey [2] states that only few solutions (such as [3], [4], [5], [6]) have been proposed to tackle this problem from an adaptive point of view. In fact, none of the aforementioned papers try to exploit a specific model structure as the basis of the adaptivity properties of MPC.

In this work, we propose a concept of data-driven MPC which is based on a finite set of *orthonormal basis functions* (OBFs). The first contribution to relate MPC and OBFs can be found in [7]. This work uses the filtering properties of the OBFs for designing a state observer and a fault tolerant controller. The utilization of OBF model structure to guarantee robustness properties of an MPC scheme has already been attempted in the work of [8]. Unlike these two works (and their continuations), we propose a direct utilization of *state-space* (SS) realizations of an OBF model structure for MIMO MPC. This model structure proves to be attractive in terms of adaptivity properties for a control scheme. Namely, it is accompanied with a well-defined stochastic framework for conducting system identification, it has a linear in the parameter property, and it is supported by important results originating from Kolmogorov to efficiently characterize variations of the system dynamics [9], [10]. We utilize these properties to formulate an adaptive MPC scheme which is tailored to capture changes in the plant dynamics in the closed-loop setting. The goal is to maintain the control performance after the MPC has been commissioned. The adaptation itself is achieved by iterative re-identification of the model coefficients. In a more general adaptation setting, the OBF model structure also offers to update its dynamical structure in terms of the basis function.

The paper is organized as follows. The formulation of *linear time invariant* (LTI) model structures with OBFs and the corresponding system theoretical aspects are presented in Section III. Afterwards, procedures for iterative model coefficients estimation are described in Section IV. Section V explains the integration of the model structure into the predictive control scheme. The concept of data-driven MPC is summarized in Section VI. Lastly, in Section VII, the proposed concept is tested on a benchmark model of a binary distillation column. Conclusions are drawn in Section VIII.

This research is financially supported by the SMART project which is a joint consortium of TU Eindhoven, KU Leuven, and IPCOS.

A.A.Bachnas, S.Weiland, and R. Tóth are with the Control System group of Electrical Engineering Department, TU Eindhoven, 5612 AJ Eindhoven, The Netherlands, emails:{a.a.bachnas,s.weiland,r.toth}@tue.nl

II. Notation

Two ways of denoting signal samples will be used. Let $p(k)$ denote the value of a vector valued signal $p : \mathbb{Z} \to \mathbb{R}^{n_p}$ at time instant k. Introduce the symbol $\mathsf{p}_N^k \in \mathbb{R}^{N \times n_p}$ for a matrix of N past signal samples $\{p(i)\}_{i=k-N+1}^{k}$:

$$\mathsf{p}_N^k = \begin{bmatrix} p(k-N+1) & p(k-N+2) & \dots & p(k) \end{bmatrix}^\top. \quad (1)$$

The other symbol is $\breve{\mathsf{p}}_k^N \in \mathbb{R}^{n_p N}$ which is the vector collection of future predictions of the signal $\{p(k+i|k)\}_{i=0}^{N}$ from data obtained up to time instant k:

$$\breve{\mathsf{p}}_k^N = \begin{bmatrix} p^\top(k|k) & p^\top(k+1|k) & \dots & p^\top(k+N|k) \end{bmatrix}^\top. \quad (2)$$

III. The LTI-OBF model structure

The LTI-OBF model structure is based on a specific series expansion representation of an LTI system that is constructed from a finite set of OBFs. The formulation of the model structure in the state-space form is straightforward and the underlying properties of the structure are attractive for model adaptation.

A. Orthonormal basis of $\mathcal{RH}_2$

The OBFs used in the LTI-OBF model is defined as $\{\phi_i(z)\}_{i=1}^{n_\mathrm{b}} \in \mathcal{RH}_2$, which is a subset (truncation) of a complete orthonormal basis $\{\phi_i(z)\}_{i=1}^{\infty}$ of $\mathcal{RH}_2$, the *Hardy space* of complex valued functions that are rational with real valued coefficients, strictly proper, analytic in the exterior of the unit disc, and square integrable over the unit circle. The

Hardy space is a separable Hilbert space with inner product defined as:

$$\langle F_1(z), F_2(z)\rangle_{\mathcal{RH}_2} = \frac{1}{2\pi}\int_{-\pi}^{\pi} F_1(e^{iw})F_2^*(e^{iw})dw. \quad (3)$$

B. Series expansion representations via OBFs

Given a complete orthonormal basis $\{\phi_i(z)\}_{i=1}^{\infty} \in \mathcal{RH}_2$, the transfer function $F(z) \in \mathcal{RH}_2^{n_\mathrm{y}\times n_\mathrm{u}}$ (space of $n_\mathrm{y}\times n_\mathrm{u}$ matrices with elements in $\mathcal{RH}_2$) of any strictly proper asymptotically stable *multi-input multi-output* (MIMO) LTI system can be written as:

$$F(z) = \sum_{i=1}^{\infty} \mathsf{w}_i \phi_i(z), \quad (4)$$

where $\mathsf{w}_i \in \mathbb{R}^{n_\mathrm{y}\times n_\mathrm{u}}$ is a matrix of expansion coefficients whose (m,n)-th entry is given by:

$$\mathsf{w}_i^{m,n} = \langle \phi_i(z), F_{m,n}(z)\rangle_{\mathcal{RH}_2}. \quad (5)$$

Here, $F_{m,n}(z)$ denotes the (m,n)-th entry of $F(z)$. We are interested in the truncations of (4) w.r.t. the first n_b basis functions:

$$F_{\mathrm{OBF}}(z) = \sum_{i=1}^{n_\mathrm{b}} \mathsf{w}_i \phi_i(z). \quad (6)$$

Any such truncation incurs an error $F_{\mathrm{n_b}}(z) := F(z) - F_{\mathrm{OBF}}(z)$, where the error norm, that is induced by the inner product, is defined by:

$$\| F^{m,n}(z) - F_{\mathrm{OBF}}^{m,n}(z)\|_{\mathcal{RH}_2}^2 = \sum_{i=n_\mathrm{b}+1}^{\infty} (\mathsf{w}_i^{m,n})^2. \quad (7)$$

Clearly the error (7) depends on the choice of the OBFs $\{\phi_i(z)\}_{i=1}^{n_\mathrm{b}}$. Note that, the series expansion representation (4) is given in term of scalar basis, for MIMO basis see [9].

C. Construction and realizations of OBFs

The OBFs considered in this paper are the *Takenaka-Malmquist* functions:

$$\phi_i(z) = \frac{\sqrt{1-|\lambda_i|^2}}{z-\lambda_i}\prod_{j=1}^{i-1}\frac{1-\lambda_j^* z}{z-\lambda_j}, \quad (8)$$

where $\{\lambda_1,\ldots,\lambda_i\} \in \mathbb{D}$ are complex numbers inside the unit disc. In addition, we define the *Blaschke product*:

$$G_b(z) = \prod_{j=1}^{n_\mathrm{b}} \frac{1-\lambda_j^* z}{z-\lambda_j}, \quad (9)$$

where n_b is the order of the all-pass filter $G_b(z)$ and $\{\lambda_i\}_{i=1}^{n_\mathrm{b}} \subset \mathbb{D}$ can be seen as the poles of the filter. Suppose that $A_\mathrm{b} \in \mathbb{R}^{n_\mathrm{b}\times n_\mathrm{b}}, B_\mathrm{b} \in \mathbb{R}^{n_\mathrm{b}\times 1}, C_\mathrm{b} \in \mathbb{R}^{1\times n_\mathrm{b}}, D_\mathrm{b} = 0$ realizes $G_b(z)$ in the sense that it is jointly input-output balanced. Then, it has been shown in [9] that (6) admits a state-space realization of the form:

$$x(k+1) = \underbrace{\begin{bmatrix} A_\mathrm{b} & \ldots & 0 \\ \vdots & \ddots & \vdots \\ 0 & \ddots & A_\mathrm{b}\end{bmatrix}}_{A\in\mathbb{R}^{n_\mathrm{g}\times n_\mathrm{g}}} x(k) + \underbrace{\begin{bmatrix} B_\mathrm{b} & \ldots & 0 \\ \vdots & \ddots & \vdots \\ 0 & \ddots & B_\mathrm{b}\end{bmatrix}}_{B\in\mathbb{R}^{n_\mathrm{g}\times n_\mathrm{u}}} u(k)$$

$$y(k) = \theta^\top x(k) \quad (10)$$

where $n_\mathrm{g} = n_\mathrm{b}\cdot n_\mathrm{u}$, $x(k) \in \mathbb{R}^{n_g}$ is the state of the filter banks $\{\phi_i(z)\}_{i=1}^{n_\mathrm{b}}$, $u(k) \in \mathbb{R}^{n_\mathrm{u}}$ and $y(k) \in \mathbb{R}^{n_\mathrm{y}}$ are the inputs and the outputs of the system represented by (6) respectively, and the coefficient $\theta \in \mathbb{R}^{n_\mathrm{g}\times n_\mathrm{y}}$ is *1-1* related to the expansion coefficients $\{\mathsf{w}_i\}_{i=1}^{n_\mathrm{b}}$, i.e. there exists a bijection between θ in (10) and $\{\mathsf{w}_i\}_{i=1}^{n_\mathrm{b}}$ in (6). In fact, by using the shift operators q, one can show that the state in (10) is generated by:

$$x(k) = [\phi_1(q)u_1(k) \ \ldots \ \phi_{n_\mathrm{b}}(q)u_1(k)\ldots \\ \phi_1(q)u_{n_\mathrm{u}}(k)\ldots \ \phi_{n_\mathrm{b}}(q)u_{n_\mathrm{u}}(k)]^\top. \quad (11)$$

A more detailed description of the OBFs of the type (8) and their properties can be found in Chapter 2 and 10 of [9].

D. Optimality of the selected OBFs

Suppose that a system with $F(z) \in \mathcal{RH}_2$ has been modeled by (6) using the OBFs of (8). Introduce $\Phi_{n_\mathrm{b}} \subset \mathcal{RH}_2$ as the subspace spanned by $\{\phi_i(z)\}_{i=1}^{n_\mathrm{b}}$ and $\overline{\Phi}_{n_\mathrm{b}} \subset \mathcal{RH}_2$ as its orthogonal complement. According to [9], [11], the error $F_{\mathrm{n_b}} \in \overline{\Phi}_{n_\mathrm{b}}$ has exponential rate of convergence (with rate $\rho \geq 0$) since

$$\|F_{\mathrm{n_b}+l\mathrm{n_b}}^{m,n}\|_{\mathcal{RH}_2} \approx \rho^l \|F_{\mathrm{n_b}}^{m,n}\|_{\mathcal{RH}_2}, \ \ \forall\, l \in \mathbb{N}. \quad (12)$$

In order to improve the convergence rate of the approximate model (6), we need to select $\{\lambda_i\}_{i=1}^{n_\mathrm{b}}$ in (9) to minimize

$$\rho(\{\lambda_i\}_{i=1}^{n_\mathrm{b}}) := \max_{z\in\Omega}\prod_{i=1}^{n_\mathrm{b}}\left|\frac{z-\lambda_i}{1-\lambda_i^* z}\right|, \quad (13)$$

with $\Omega \subset \mathbb{D}$ is the set of nominal poles of $F(z)$. This procedure is also known as the inverse *kolmogorov n-width* (KnW) problem and the methods for optimal selection of the all-pass filter poles can be found in [11], [12].

E. Adaptation of the LTI-OBF model

In the scope of this work, we are interested in adapting the model $F_{\mathrm{OBF}}(z)$ in case the underlying system $F(z) \in \mathcal{RH}_2$, which is modeled during the commissioning stages, changes into a different system $\tilde{F}(z) \in \mathcal{RH}_2$. The adaptation goal is to minimize the approximation error of the model w.r.t. the new system $\|\tilde{F}_{\mathrm{n_b}}^{m,n}\|_{\mathcal{RH}_2}$ for all m,n input-output channel. This can be done by executing different levels of adaptation:

1) If $\|\tilde{F}_{\mathrm{n_b}}^{m,n}\|_{\mathcal{RH}_2} \leq \|F_{\mathrm{n_b}}^{m,n}\|_{\mathcal{RH}_2}$, then the adaptation is governed by re-estimating new coefficient $\tilde{\theta}$ of (10).
2) If $\|\tilde{F}_{\mathrm{n_b}}^{m,n}\|_{\mathcal{RH}_2} \geq \|F_{\mathrm{n_b}}^{m,n}\|_{\mathcal{RH}_2}$, but $\|\tilde{F}_{\mathrm{n_b}+\mathrm{ln_b}}^{m,n}\|_{\mathcal{RH}_2} \leq \|F_{n_\mathrm{b}+ln_\mathrm{b}}^{m,n}\|_{\mathcal{RH}_2}$, then the adaptation is conducted by including more OBFs via repeating the poles of $G_b(z)$ for l times in the expansion (6) and realization (10).
3) In case the number of repetition l in the second level becomes relatively large, re-selection of the OBFs is conducted by solving the inverse KnW problem mentioned in Section III-D to maintain low approximation error as well as low model complexity.

This paper only covers the first level of adaptation. For the second item, longer expansion of (6) can be deliberately used to maintain arbitrarily low approximation error. By doing this, it is possible to utilize the change of coefficient $\tilde{\theta}$ as a detection tool of growing approximation error by employing *hypothesis test* such as mentioned in [13].

IV. Coefficient Estimation of LTI-OBF models

Estimation of expansion coefficients of the OBF model structure is often accomplished as a parameter estimation problem in the *prediction error minimization* (PEM) setting with a well-defined stochastic framework [14], [9]. Similar to the FIR model structure in PEM, this is an attractive model structure due to linearity in the model parameters resulting in an analytic solution of the identification problem.

A. The PEM identification setting

It is assumed that a data-sequence of input and output signals $\mathcal{D}_N^{(k)} = \{u(\tau), y(\tau)\}_{\tau=k-N+1}^{k}$ generated by a system $F(z) \in \mathcal{RH}_2^{n_y \times n_u}$:

$$y(k) = F(q)u(k) + v(k) \tag{14}$$

is available, where $F(q)$ is the transfer operator form of $F(z)$, with q being the time shift operator, and $v(k)$ is a zero mean stationary noise sequence with rational spectra. In the *output error* (OE) setting of (14), the estimate of coefficient θ of (10) for a given set of basis $\{\phi_i(z)\}_{i=1}^{n_b}$ is obtained by minimizing the *least-squares* (LS) identification criterion:

$$\hat{\theta} = \arg\min_{\theta} \underbrace{\frac{1}{N}\sum_{t=1}^{N} \varepsilon(k,\theta)^2}_{V_N(\theta)} \tag{15a}$$

$$\varepsilon(k,\theta) := y(k) - \hat{y}(k\,|\,k-1;\theta) \tag{15b}$$

of the one step-ahead prediction error $\varepsilon(k,\theta)$ of the model output $\hat{y}(k\,|\,k-1;\theta) = \hat{\theta}x(k)$. Introduce θ^* as the coefficient of the SS representation of the truncated expansion of $F(z)$ in terms of (6). If the input sequence u is persistently exciting w.r.t. the filter (10), then $\hat{\theta} \to \theta^*$, with probability 1 as $N \to \infty$. More on the properties of PEM based identification with LTI-OBF models can be found in Chapter 4 and 5 of [9].

B. Iterative estimation of the model coefficients

To accommodate adaptivity, the coefficient θ must be estimated at each time instant k, and will be further denoted by $\hat{\theta}_k$. Two methods which are based on the analytic solution of (15), namely the weighted and recursive LS estimation, are presented for this purpose. In order to capture possible changes of the system dynamics, the identification will be conducted iteratively in a closed loop setting. Unfortunately, this implies that $v(k)$ and $u(k)$ are correlated. Without any additional modification of (15), such as an *instrumental-variables* (IV) scheme [15], this means that there will be an estimation bias on the coefficient $\hat{\theta}_k$. For the sake of simplicity, the incorporation of such schemes in the iterative identification will be covered in future work.

1) Weighted LS estimation: Using weighting approach, the estimation problem is solved by:

$$\hat{\theta}_k^{\mathrm{LS}} = ((\mathsf{x}_N^k)^\top W_{\mathrm{LS}} \mathsf{x}_N^k)^{-1} (W_{\mathrm{LS}} \mathsf{x}_N^k)^\top \mathsf{y}_N^k, \tag{16}$$

where the tuning (hyper) parameter for this method is the number of the considered past data N and the exponential weighting $W_{\mathrm{LS}} = \mathrm{diag}\big(\{\frac{\beta^k}{\beta^N}\}_{k=1}^{N}\big)$ with $\beta \in \mathbb{R}_{(0,\infty)}$. The parameter N should be chosen to be larger than the settling time of the slowest step response of the system dynamics. A high value of N can reduce the estimation variance which is caused by the noise, but result in slow adaptation speed of the model. This situation can be remedied by the weighting W_{LS} that penalizes the effect of old data as proposed in [14]. A sensible value of β is in the range of $(0, 20]$.

2) Recursive LS estimation : In this method, the estimation of coefficient $\hat{\theta}_k$ is based on variables that can be considered as the memory of the estimate [14]. The update strategy requires computation of:

$$\hat{\theta}_k^{\mathrm{RLS}} = \hat{\theta}_{k-1}^{\mathrm{RLS}} + L(k)\varepsilon^\top(k), \tag{17a}$$

$$L(k) = \frac{P(k-1)x(k)}{W_{\mathrm{RLS}} + x^\top(k)P(k-1)x(k)}, \tag{17b}$$

$$P(k) = \frac{1}{W_{\mathrm{RLS}}}\left(P(k-1) - \frac{P(k-1)x(k)x^\top(k)P(k-1)}{W_{\mathrm{RLS}} + x^\top(k)P(k-1)x(k)}\right). \tag{17c}$$

where $L(k) \in \mathbb{R}^{n_g}$ is the gain matrix, and $P(k) \in \mathbb{R}^{n_g \times n_g}$ is the conditional covariance matrix of the estimation error. The gain matrix $L(k)$ governs the rate of change of the estimated coefficient and can be seen as the gradient of the parameter estimate. The hyper parameter of this estimation method is the weight $W_{\mathrm{RLS}} \in \mathbb{R}_{(0,1)}$ which also known as the forgetting factor. The value of $W_{\mathrm{RLS}} \approx 1$ is a reasonable choice to allow continuous update on model coefficients. The recursive algorithm requires initial values of $P(k-1)$ and $\hat{\theta}_{k-1}$. Typically, the initial values are obtained by starting the recursion at a time instant k_0 with

$$P(k_0 - 1) = \left[\sum_{\tau=0}^{k_0-1} x(\tau)x^\top(\tau)\right]^{-1}, \tag{18a}$$

$$\hat{\theta}_{k_0-1}^{\mathrm{RLS}} = P(k_0 - 1)\sum_{\tau=0}^{k_0-1} x(\tau)y(\tau)^\top. \tag{18b}$$

C. Calculation of the current state of the filters

Note that both the weighted and the recursive LS estimation require the current state value $x(k)$. From (11), it can be seen that the state trajectory is determined by the inputs $u(k)$ that is passed through the filter banks $\{\phi_i(q)\}_{i=1}^{n_b}$. Hence, $x(k)$ can be obtained by selecting a past time instant $k_0 \ll k$ and then compute the current state $x(k)$ recursively by:

$$x(k) = A^{k-k_0}x(k_0) + \sum_{l=0}^{k-k_0-1} A^l B u(k_0 + l). \tag{19}$$

Since the filter is stable, the effect of the initial state $x(k_0)$ gradually dies out. Hence, considering $x(k_0) = 0$ will not result in a cumulative error in the value of $x(k)$. The next state $x(k+1) = Ax(k) + Bu(k)$ can be computed directly from the current input $u(k)$. As an additional note, the state $x(k)$ can also be estimated w.r.t. the input-output data. An *extended Kalman filter* can be designed to jointly estimate the current state $x(k)$ together with the variation of coefficient θ_k. This method is not explored for this work since the design (stability) of the filter is not trivial and it is computationally heavier compared to a direct calculation of (19).

V. OBF based MPC Formulation

This section describes the integration of the OBF model structure into an MPC scheme. The predictor form of the OBF model is formulated first and then the MPC formulation is developed.

A. Predictor form of the OBF model

The SS representation (10) of the OBF model structure allows a similar formulation as in [16]. The predicted outputs of the system (up to the prediction horizon H_p) are constructed based on a linear combination of the future state trajectory of the filter that is described by input increments $\Delta u(k) = u(k) - u(k-1)$:

$$\check{\mathsf{x}}_k^{H_p} = \underbrace{\begin{bmatrix} A \\ \vdots \\ A^{H_\mathrm{u}} \\ \vdots \\ A^{H_p} \end{bmatrix}}_{\Psi\in\mathbb{R}^{H_p n_\mathrm{g}\times n_\mathrm{g}}} x(k) + \underbrace{\begin{bmatrix} B \\ \vdots \\ \sum_{l=0}^{H_\mathrm{u}-1} A^l B \\ \vdots \\ \sum_{l=0}^{H_p-1} A^l B \end{bmatrix}}_{\Upsilon\in\mathbb{R}^{H_p n_\mathrm{g}\times n_\mathrm{u}}} u(k-1) + \underbrace{\begin{bmatrix} B & \dots & 0 \\ \vdots & \ddots & \vdots \\ \sum_{l=0}^{H_\mathrm{u}-1} A^l B & \dots & B \\ \vdots & \vdots & \vdots \\ \sum_{l=0}^{H_p-1} A^l B & \dots & \sum_{l=0}^{H_p-H_\mathrm{u}} A^l B \end{bmatrix}}_{\Theta\in\mathbb{R}^{H_p n_\mathrm{g}\times H_\mathrm{u} n_\mathrm{u}}} \Delta\check{\mathsf{u}}_{k-1}^{H_u-1}. \quad (20)$$

where $H_u \leq H_p$ is the control horizon, $\check{\mathsf{x}}_k^{H_p}$ is the vectorized form of the predicted state trajectory, and $\Delta\check{\mathsf{u}}_{k-1}^{H_u-1}$ is the vectorized form of future input increment sequence. The formulation of the state as a function of $\Delta u(k)$ is chosen to generate integral action in the controller. The H_p step-ahead predicted output $y(k+i|k)$ can be formulated as:

$$\check{\mathsf{y}}_k^{H_p} = \underbrace{\begin{bmatrix} \hat{\theta}_k^\top & \dots & 0 \\ \vdots & \ddots & \vdots \\ 0 & \ddots & \hat{\theta}_k^\top \end{bmatrix}}_{\Xi(k)\in\mathbb{R}^{H_p n_\mathrm{y}\times H_p n_\mathrm{g}}} \check{\mathsf{x}}_k^{H_p}. \quad (21)$$

where $\hat{\theta}_k$ is the coefficient that is obtained from either one of the two aforementioned estimation approaches (16) or (17). It can be seen that the predicted outputs:

$$\check{\mathsf{y}}_k^{H_p} = \Xi(k)\Psi x(k) + \Xi(k)\Upsilon u(k-1) + \Xi(k)\Theta\Delta\check{\mathsf{u}}_{k-1}^{H_u-1} \quad (22)$$

are constructed based on past data (governed by $\Xi(k)$), present data (shown by the current state $x(k)$ and input $u(k-1)$), and the future input increment sequence ($\Delta\check{\mathsf{u}}_{k-1}^{H_u-1}$).

B. Cost function and optimization problem

The formulation of the MPC scheme is based on the standard quadratic cost function that penalizes deviation of the output w.r.t. a known reference ($\check{\mathsf{r}}_k^{H_p}$) and the rate of change of the input $\Delta\check{\mathsf{u}}_{k-1}^{H_u-1}$:

$$\begin{aligned} V(k) = \ & [\check{\mathsf{y}}_k^{H_p} - \check{\mathsf{r}}_k^{H_p}]^\top Q[\check{\mathsf{y}}_k^{H_p} - \check{\mathsf{r}}_k^{H_p}] + \\ & [\Delta\check{\mathsf{u}}_{k-1}^{H_u-1}]^\top R[\Delta\check{\mathsf{u}}_{k-1}^{H_u-1}]. \end{aligned} \quad (23)$$

The weighting matrices Q and R are symmetric, positive semi-definite matrices that define the control specification. The matrix Q is used to put emphasis on a particular output according to its importance or sensitivity. The tuning matrix R is utilized to mitigate the aggressiveness of the control action. The minimization problem of $V(k)$ w.r.t. the future input increment sequence $\Delta\check{\mathsf{u}}_{k-1}^{H_u-1}$ is solved while obeying operational constraints. With prescribed range of future output, input, as well as the input increment, this task amounts to solving the optimization problem of:

$$\begin{aligned} \min_{\Delta\check{\mathsf{u}}_{k-1}^{H_\mathrm{u}-1}} \quad & V(k) \\ \text{s.t.} \quad & \mathsf{y}_{\min} \leq \check{\mathsf{y}}_\mathsf{k}^{\mathsf{H_p}} \leq \mathsf{y}_{\max}, \\ & \mathsf{u}_{\min} \leq \check{\mathsf{u}}_{\mathsf{k-1}}^{\mathsf{H_u-1}} \leq \mathsf{u}_{\max}, \\ & \Delta\mathsf{u}_{\min} \leq \Delta\check{\mathsf{u}}_{k-1}^{H_u-1} \leq \Delta\mathsf{u}_{\max}. \end{aligned} \quad (24)$$

Since the cost function of (23) and the operational constraint can be written as a quadratic and a linear function of the input increment $\Delta\check{\mathsf{u}}_{k-1}^{H_u-1}$ respectively, the optimization problem (24) is a *quadratic programming* (QP) problem, and can be solved efficiently using a wide range of available QP solvers. Stability of the proposed control scheme can be ensured by the inclusion of a terminal cost and terminal set into the control problem (24) such as described in [17]. The stability is implied if there exists a robust LTI terminal controller for all possible values of $\hat{\theta}_k$.

VI. Algorithm

The underlying concept of the proposed control scheme in terms of model adaptation and MPC formulation have been given in the previous sections. This section summarizes those procedures into Algorithm 1. After the design step, the initialization is required before the main control-identification loop can be activated. On top of this Algorithm, strategies mentioned in the Section III-E can be employed to detect growing approximation error and initialization to re-select the basis functions.

VII. Simulation study

The proposed control scheme is tested on a binary distillation column benchmark model that is based on a liquid-vapor flow configuration. The model is detailed in [18]. A linearization of the model is established for the operating condition of 0.5 and 0.95 (mole fraction) of the bottom and top composition levels respectively, with corresponding liquid and vapor flows of 521 kmol/min (kilo-mole per minute) and 664 kmol/min. The sampling time of the system is chosen to be 5 minutes while the settling time of the system is 170 minutes (34 time steps). The MIMO LTI model in deviation variables is given as follows:

$$G(z) = \begin{bmatrix} \frac{0.001357z-0.0009633}{z^2-1.528z+0.5679} & \frac{-0.0009023z+0.000597}{z^2-1.528z+0.5679} \\ \frac{0.001174z-0.0009952}{z^2-1.528z+0.5679} & \frac{-0.0003762z+0.0002929}{z^2-1.528z+0.5679} \end{bmatrix}.$$

This represents a 2x2 LTI system with liquid and vapor flow as the inputs (manipulated variables) and bottom and top composition as the output (controlled variables) respectively.

Algorithm 1 MPC-OBF scheme

Require:

- Selected basis poles $\{\lambda_i\}_{i=1}^{n_\mathrm{b}}$ and their associated realization (A,B) according to (10).
- Hyper parameters for LS estimation (N,W_{LS}) or RLS estimation (W_{RLS}).
- Control parameters H_p, H_u, Q and R.

1: Given measurement data $\mathcal{D}_N^{(k)}$,
- Compute state trajectory $\{x(\tau)\}_{k_0}^{k}$ via (19).
- LS approach: Generate matrix x_N^k according to (1).
- RLS approach: Generate the initial values of $P(t_0)$ and $\hat{\theta}_{t_0}$ (or set them to 0 with proper dimensions) and propagate up to $P(k-1)$ and $\hat{\theta}_{k-1}$ based on (18).

2: Calculate state $x(k)$ based on $x(k-1)$ and $u(k)$.

3: Do coefficient estimation:
- LS approach: Calculate coefficient $\hat{\theta}_k$ based on (16).
- RLS approach: Calculate the gain matrix $L(k)$ and the current coefficient $\hat{\theta}_k$ based on (17) then update matrix $P(k)$.

4: Solve the QP optimization problem of (24) to obtain $\Delta u(k)$.

5: Apply input $u(k)$.

6: **Wait** New measurement of output $y(k+1)$.

7: Set $k \leftarrow k+1$.

8: Go to 2.

TABLE I: Open-loop validation result for both approaches.

	Bottom product composition (y_1)	Top product composition (y_2)
	BFR	BFR
LS-approach	94.88 %	87.18 %
RLS-approach	89.81 %	84.26 %

The generated measurements from this system are corrupted by a discrete-time output additive white noise with *signal to noise ratio* (SNR) of 15 dB. The MPC-OBF scheme will be designed and commissioned on this system with $n_\mathrm{b} = 4$ basis functions that are generated from the poles of the system i.e. $\| F_{n_\mathrm{b}}^{m,n}(z) \|_{\mathcal{RH}_2} = 0$. After the commissioning of the MPC, the plant-model mismatch will be induced as an effect of a rotation matrix:

$$G_{\mathrm{new}}(z) = \begin{bmatrix} \cos(\alpha(k)) & -\sin(\alpha(k)) \\ \sin(\alpha(k)) & \cos(\alpha(k)) \end{bmatrix} G(z), \qquad (25)$$

where $-\pi/5 < \alpha(k) < 0$ is the rotation coefficient at time instant k. Different rates of change of $\alpha(k)$ such as abrupt and slow changes are considered in the experiment. The goal of this study is to test the ability of the MPC-OBF scheme to track the change of the system while maintaining low deviation from the given reference point. Since the rotation matrix only induces changes on the output side, adaptation in term of model coefficient $\hat{\theta}_k$ is sufficient in this example.

A. Initial observation and open-loop validation

An off-line experiment (study) has been conducted which corresponds to the commissioning stage of the MPC where

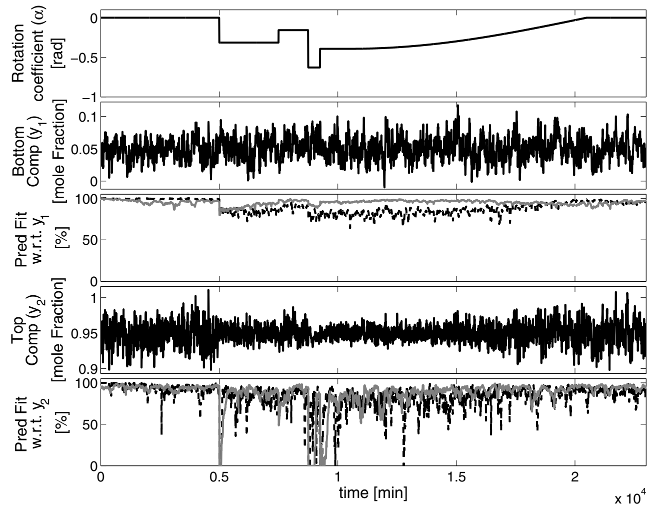

Fig. 1: Validation performance of the selected hyper parameters in the open-loop setting. LS approach (solid grey line), RLS approach (dashed black line).

the hyper parameters of the estimation and the control parameters are selected. In this experiment, the system is excited with Gaussian white noise input with standard deviation of 10 kmol/min. The length of the simulation study is 23000 minutes (383 hours). It is important to note that this experimental length is not the required time to obtain the model. Instead, the length is chosen such that the estimation capabilities of the model can be assessed with respect to various rotation scenarios. The H_p-step ahead prediction for each time instant k will be calculated to display prediction capabilities of the obtained model. The result of this experiment can be seen in Fig. 1 and Table I in terms of average *best fit ratio* (BFR). These results correspond to the selected hyper parameters of $N = 239$, $W_{\mathrm{LS}} = \mathrm{diag}\big(\{\frac{4.5^k}{4.5^N}\}_{k=1}^{N}\big)$, and $W_{\mathrm{RLS}} = 0.97$ which are obtained via the gridding of the parameter space. For the controller, we select the values of $H_\mathrm{u} = H_\mathrm{p} = 34$ which are based on the slowest subprocess of the system. Fig. 1 shows that the introduced rotation has a shrinking effect on the top output channel, thus making the SNR of the top output channel lower than the bottom one. Hence, the value of $Q = \mathrm{diag}(6, 7)$ and $R = \mathrm{diag}(0.01, 0.01)$ are chosen to put slightly more emphasis on the top output channel.

B. Closed-loop experiment

With the parameters available from Section VII-A, the MPC-OBF is commissioned on the system. The control task is to follow a set point of $r_1 = 0.02$ and $r_2 = 0.98$ for each of the output channels under the effect of rotation factor that is depicted in Fig. 1. Four different cases are considered for the closed-loop experiment. The first case is the Oracle-MPC where the predictive model is equal to the true system dynamics. The result of the Oracle-MPC will also serve as a benchmark on the best achievable result on the selected control parameter. The second case considers a fix model for the whole experiment (Fixed-MPC). The third and the fourth cases are the MPC-OBF with either LS or RLS adaptation.

TABLE II: Closed-loop performance of the investigated MPC approaches with respect to the given reference

	Bottom product composition (y_1)		Top product composition (y_2)	
	MSE	BFR	MSE	BFR
Fixed-MPC	$7.64 \cdot 10^{-5}$	70.75 %	$3.67 \cdot 10^{-5}$	79.76 %
Oracle MPC	$1.05 \cdot 10^{-6}$	95.87 %	$2.75 \cdot 10^{-6}$	94.38 %
MPC-OBF LS	$1.37 \cdot 10^{-5}$	87.45 %	$7.33 \cdot 10^{-6}$	90.92 %
MPC-OBF RLS	$1.17 \cdot 10^{-5}$	88.34 %	$5.96 \cdot 10^{-6}$	91.79 %

The result of the closed-loop experiment, with their BFR and *mean-squared error* (MSE), can be seen in Fig. 2 and in Table II.

From these results, it can be seen that the Fixed-MPC cannot give proper reaction to the change of the system since the current condition of the system is unknown to the model. On the other hand, the MPC-OBF which is based on an adaptive model can still follow the reference in both abrupt or slow rotation scenarios. From Table II, it can be seen that the recursive approach slightly outperforms the least-squares approach. This result is the opposite of the open-loop simulation result (Table I) where the adaptations of the system dynamics were performed better by the least-squares approach. The explanation of this behavior is the informativeness of the data set. In the open-loop setting (Fig. 1), the excitation signals in the form of white noise input contain rich information and hence the analytic computation based on a long data set will produce better results. In contrary in the closed-loop setting, the input excitation is limited which results in limited information in the data set.

VIII. Conclusion and Future Work

The concept of a data-driven adaptive predictive control scheme based on an OBF model structure has been presented. The structure of the model can be exploited to offer adaptation abilities w.r.t. changes in the controlled system dynamics. The simulation study shows promising results where the iterative model adaptations are able to mitigate the plant-model mismatch and hence improve control performance. In future works, a thorough explanation and inclusion of several items such as closed loop recursive identification via an IV scheme, persistency excitation of the control action, a proof of stability, and a hypothesis test for the necessity of re-optimizing OBFs will be explored to complete the whole proposed MPC scheme.

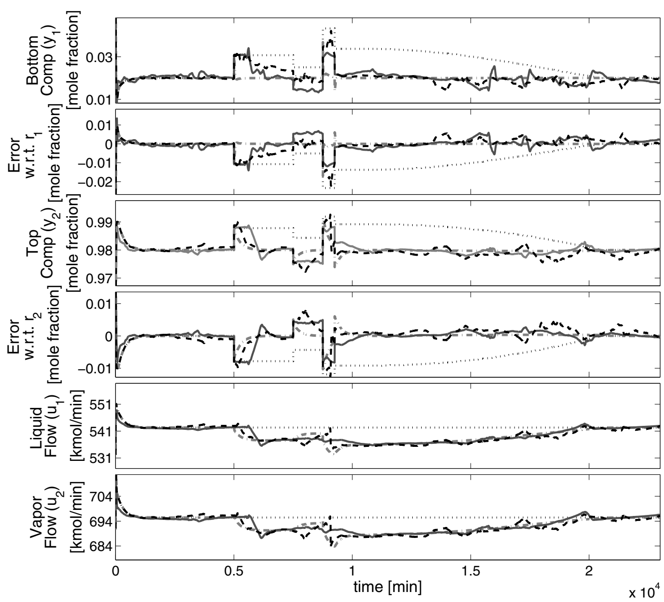

Fig. 2: Performance of four different cases of predictive controller under rotation scenario. Fixed MPC (dotted black line), Oracle MPC (dash-dotted grey line), MPC-OBF with LS estimation (solid grey line), MPC-OBF with RLS estimation (dashed black line).

References

[1] S.J. Qin and T. Badgwell. A survey of industrial model predictive control technology. *Control engineering practice*, 11(7):733–764, 2003.

[2] D.Q. Mayne. Model predictive control: Recent developments and future promise. *Automatica*, 50(12):2967–2986, 2014.

[3] G. Marafioti, R.R. Bitmead, and M. Hovd. Persistently exciting model predictive control. *International Journal of Adaptive Control and Signal Processing*, 28(6):536–552, 2014.

[4] H. Genceli and M. Nikolaou. New approach to constrained predictive control with simultaneous model identification. *AIChE journal*, 42(10):2857–2868, 1996.

[5] M. Tanaskovic, L. Fagiano, R. Smith, and M. Morari. Adaptive receding horizon control for constrained MIMO systems. *Automatica*, 50(12):3019–3029, 2014.

[6] T.A.N. Heirung, B. Foss, and B.E. Ydstie. MPC-based dual control with online experiment design. *Journal of Process Control*, 32:64–76, 2015.

[7] S.C. Patwardhan and S.L. Shah. From data to diagnosis and control using generalized orthonormal basis filters. part I: Development of state observers. *Journal of Process Control*, 15(7):819–835, 2005.

[8] A. Douik, J. Ghabi, and H. Messaoud. Robust predictive control using a GOBF model for MISO systems. *International Journal of Computers, Communications & Control*, 2(4):355–366, 2007.

[9] P. S. C. Heuberger, P. M. J. Van den Hof, and Bo Wahlberg. *Modeling and Identification with Rational Orthonormal Basis Functions*. Springer-Verlag, 2005.

[10] B. Ninness and F. Gustafsson. A unifying construction of orthonormal bases for system identification. *IEEE Transactions on Automatic Control*, 42(4):515–521, 1997.

[11] T Oliveira e Silva. A n-width result for the generalized orthonormal basis function model. In *Proc. of the 13th IFAC World Congress*, volume 1, pages 375–380, 1996.

[12] R. Tóth, P.S.C. Heuberger, and P.M.J. Van den Hof. Asymptotically optimal orthonormal basis functions for LPV system identification. *Automatica*, 45(6):1359–1370, 2009.

[13] A. Mesbah, X. Bombois, M. Forgione, J.H.A. Ludlage, P.E. Modén, H.Hjalmarsson, and P.M.J. Van den Hof. A unified experiment design framework for detection and identification in closed-loop performance diagnosis. In *Proc. of the 51st IEEE Annual Conference on Decision and Control*, pages 2152–2157, 2012.

[14] L. Ljung. *System Identification, theory for the user*. Prentice-Hall, 2nd edition, 1999.

[15] P. Young, H. Garnier, and M. Gilson. Simple refined IV methods of closed-loop system identification. In *Proc. of the 15th IFAC Symposium on System Identification, SYSID 2009*, pages 284–289, 2009.

[16] J.M. Maciejowski. *Predictive control: with constraints*. Pearson education, 2002.

[17] D.Q. Mayne, J.B. Rawlings, C.V. Rao, and P.O.M Scokaert. Constrained model predictive control: Stability and optimality. *Automatica*, 36(6):789–814, 2000.

[18] S. Skogestad. Dynamics and control of distillation columns: A tutorial introduction. *Chemical Engineering Research and Design*, 75(6):539–562, 1997.